Polymer Chemistry

Accepted Manuscript

This is an *Accepted Manuscript*, which has been through the Royal Society of Chemistry peer review process and has been accepted for publication.

Accepted Manuscripts are published online shortly after acceptance, before technical editing, formatting and proof reading. Using this free service, authors can make their results available to the community, in citable form, before we publish the edited article. We will replace this *Accepted Manuscript* with the edited and formatted *Advance Article* as soon as it is available.

You can find more information about *Accepted Manuscripts* in the Information for Authors.

Please note that technical editing may introduce minor changes to the text and/or graphics, which may alter content. The journal's standard Terms & Conditions and the Ethical guidelines still apply. In no event shall the Royal Society of Chemistry be held responsible for any errors or omissions in this *Accepted Manuscript* or any consequences arising from the use of any information it contains.

ROYAL SOCIETY OF CHEMISTRY

www.rsc.org/polymers

Journal Name

ARTICLE

Ultrafast Diffusion-Controlled Thiol-Ene Based Crosslinking of Silicone Elastomers with Tailored Mechanical Properties for Biomedical Applications

Received 00th January 20xx,
Accepted 00th January 20xx

DOI: 10.1039/x0xx00000x

www.rsc.org/

Khai D. Q. Nguyen,[a,b] William V. Megone,[a,b] Dexu Kong[a,b], and Julien E. Gautrot*[a,b]

Polysiloxanes are commonly used in a wide range of applications, but their crosslinking is typically relatively slow, requires metal catalysts (for hydrosilylation or to catalyse condensation) and depends on storage and curing conditions (humidity level). Thiol-ene "click" chemistry, on the other hand, is a promising strategy to post-functionalise and cross-link polymers or to introduce different biofunctionalities for applications in the biomedical field. In the present work, we explore the use of the photo-initiated thiol-ene reaction to cross-link a side-chain thiol-functionalised poly(dimethylsiloxane) (PDMS) with telechelic vinyl-PDMS chains at ambient temperature. We investigate the impact of different curing parameters on the network properties and gelation kinetics, using *in-situ* photo-rheology. It is shown that the curing reaction occurs rapidly and very efficiently even in the presence of oxygen in the system. Whilst the mechanical properties of the cross-linked networks are strongly affected by the ratios between thiol and alkene moieties, the molecular weight, and therefore viscosity, of starting macromonomers and UV light intensity showed very small variation in the resulting storage moduli of the formed PDMS networks. The potential of using such materials in biomedical applications and cell culture were highlighted by the good cytocompatibility of thiol-ene PDMS substrates with varying mechanical properties. In addition, by utilising remaining thiol-moieties in the cross-linked networks, strong adhesion between thiol-ene matrices and the acrylate pre-treated glass surfaces was established, in mild conditions. These findings indicate an ability to systematically tailor the mechanical properties of the resulting networks whilst manipulating their surface functionalities, attractive features for a range of applications including 3D printing, microfabrication and cell culture.

Introduction

Silicones such as polydimethylsiloxane (PDMS) are a major class of organo-silicon synthetic materials based on chains of alternating silicon and oxygen atoms with aliphatic or aromatic substituents. These hybrid material have been used in a wide range of biomedical applications due to their unique characteristics, including physiological inertness, low toxicity, similar elasticity to soft biological tissues, good thermal and oxidative stability, optical transparency, high permeation to oxygen and their ease of fabrication[1, 2]. However, as a result of their extremely low glass transition temperature and weak intermolecular forces, PDMS exhibits very low mechanical properties at room temperature and requires a cross-linking to decrease its compliance.

The crosslinking chemistries of silicone-based materials have been well established for the past few decades[3], and can be categorised into three main chemical reactions: (1) radical reactions (thermally initiated or via photo-irradiation) between alkyl and/or alkene groups; (2) addition reactions (or hydrosilylation) between vinyls and hydride-terminated siloxanes in the presence of Platinum (or Rhodium) complexes; and (3) condensation reactions between hydroxy, and/or alkoxy, acetoxy groups in the presence of tin or titanium catalysts with moisture as a co-catalyst.

However, these crosslinking chemistries still present pitfalls that prevent their use for specific applications. The radical-based curing chemistry is normally performed at high temperatures with a need for a post-cure step to eliminate peroxide by-products or residues whilst the last two systems involve the use of metal-based toxic catalysts and are relatively slow processes with long cure times. On the other hand, the hydrophobicity and low surface energy of native PDMS can be advantageous in many applications, but is sometimes detrimental to promote strong adhesion with other materials or cells[4]. Bacteria, proteins and other biomolecules can absorb non-specifically to silicones surfaces, which can result in device failures, severe infection or undesirable circumstances (e.g. blood coagulation, platelet adhesion and activation, and discomfort associated with contact lens)[5-7] while the low surface tension characteristic of PDMS makes it difficult to adhere to other materials including glass and

[a] Institute of Bioengineering, Queen Mary, University of London, Mile End Road, London, E1 4NS, UK.
[b] School of Engineering and Materials Science, Queen Mary, University of London, Mile End Road, London, E1 4NS, UK.
E-mail: j.gautrot@qmul.ac.uk
Electronic Supplementary Information (ESI) available: Schematic of PDMS-glass bonding structure, mechanical characterisation and video of *in-situ* recording of adhesion test. See DOI: 10.1039/x0xx00000x

hydrogels. For such applications, the surface chemistry of silicone substrates needs to be activated (e.g. plasma treatment) or with the development of specific functionalization strategies[4, 8-11]. Another drawback of current curing chemistries of silicones is that they cannot be used in 3D printing technologies or for microfabrication as a result of its relatively slow reactivity. For example, Sylgard 184, the most well-known silicone materials used in different applications from engineering to biomedical fields, requires 48 h to be cured at ambient temperature or 35 min at 100°C[12].

Therefore, novel PDMS crosslinking strategies, with faster reaction rates in mild conditions are required. Such curing chemistry should for example allow silicone curing at low temperatures, resulting less structural damages of devices for a broader range of applications. Thiol-ene chemistry offers attractive features for the cross-linking of silicone materials. It does not require expensive and toxic metal catalysts yet proceeds with high efficiencies, it tolerates a wide range of functionalities, it can be activated by light at ambient temperatures and is significantly less sensitive to oxygen than conventional radical reactions[13, 14]. This makes it a particularly convenient coupling strategies for the biofunctionalisation of biomacromolecules, polymers and surfaces[15-17].

The thiol-ene reaction, as outlined in Scheme 1, is a step-growth radical processed based on the addition of a thiol-functional group (-SH) to a monomer with an ene- functional group (C=C). This reaction can be triggered by photo-generated radical initiators ($I^{\bullet}$), which abstract a proton from thiol monomers to produce thiyl radicals (steps 1.1 and 1.2). These thiyl species react with alkene monomers (step 2.1), resulting in radical alkyl intermediate that can transfer back to thiol monomers via further proton abstraction (step 2.2). In general, the cross-linking occurs almost exclusively via this mechanism, but can also occur to some extent via homopolymerization of vinyl groups. However, it was reported that transfer from alkyl radicals to thiols were significantly faster than propagation to other vinyl moieties[18, 19]. The propagation and chain transfer steps can be combined in a simplified single step (step 2), accounting for the generation of a stable crosslink. Finally, radical can be quenched during termination, via a variety of mechanisms, grouped in step 3. An important implication of this step growth mechanism is that the evolution of the molecular weight in thiol-ene systems proceeds relatively slowly, compared to chain-growth mechanisms, causing a delayed gelation, but also little shrinkage stress compared to conventional radical cross-linking systems.

Although thiol–ene reactions have been studied and applied to a variety of fields from polymer science to biochemistry[13, 14], it has not been utilized extensively in silicone chemistry. For example thiol-ene based silicone materials include low modulus dry silicone-gels[20], silicone rubbers[21], luminescent elastomers[22], macroporous cryogels[23], active ingredient incorporating microcapsules[24], thermo-sensitive electrospun fibers[25], organocatalytic gels[26], soft imprint lithorgraphy[27, 28], or resins for microfluidic devices[29]. Muller and Kunz studied the photo-initiated radical cross-linking of different α,ω-ene-terminated silicones (e.g. vinyl, allyl,norbornenyl and others) with mercapto siloxanes and discussed the role of the alkene chemical structure on the reaction enthalpy, network density and rate of reaction[18]. Cole and Bowman investigated termination mechanisms and the influence of non-reactive pendant groups on thiol-ene reaction rates[30]. Recently, Goswami et al. demonstrated an approach of heterogeneous bimodal networks as a pathway to mechanically improved systems without the addition of reinforcing fillers[31]. However, there is still a lack of understanding of the cross-linking processes and their kinetics in a broader range of molecular weight of siloxane polymers and the impact of such structures on mechanical properties and silicone design for biomedical applications.

In the present paper, we explore the role of molecular design in thiol-ene crosslinked PDMS on reaction rates and mechanical properties of the networks formed. Thiol-functionalised PDMS is crosslinked with vinyl-terminated PDMS of varying chain lengths. Extremely fast reaction rates (a few seconds) were reported, depending on the molecular weight of the starting macromonomers. The impact of monomer ratios and intensity of UV light irradiation was investigated via photo-rheology, revealing a diffusion controlled mechanism. In addition, microfabricated films of these thiol-ene silicones were used to study bonding to glass substrates, providing milder and less structural damaging methods for microfluidics fabrication. The cytocompatibility of the cross-linked materials was also examined for potential use in the field of biomedical applications.

Materials and Methods

Chemicals and materials

The α,ω-vinyl terminated polydimethylsiloxanes at different viscosities (1,000cSt; 3,500cSt ; 10,000cSt; and 100,000cSt) and poly[(mercaptopropyl)methylsiloxane] (M_n=4000-7000 g/mol; mercaptopropyl siloxane unit content is 100%) were obtained from ABCR GmbH, Germany. The poly[(mercaptopropyl)methylsiloxane] and α,ω-vinyl terminated polydimethylsiloxanes are referred to thereafter as PDMS-thiol and PDMS-vinyl, respectively. The photoinitiator 2,2-dimethoxy-2-phenylacetatophenone (DMPA) and other chemicals used in this study were purchased from Sigma-Aldrich and used as received

Preparation of UV curable resin

A mixture of PDMS-thiol 100 and PDMS-vinyl at required quantities were diluted by Diclomethane (DCM) and stirred for 5 min. A stock solution of photoinitiator, DMPA, in DCM was prepared and then added to the mixture and mixed thoroughly for an additional 15 min. Finally, the solvent, DCM, was removed from the mixture in high vacuum. Samples were kept away from any source of light during the preparation. The photoinitator, i.e. DMPA, was keept at the equivalent molar ratio of 0.1:1 with respect to that of thiol content throughout this study. All equivalent ratios were calculated based on the

molecular weight of starting materials given by the manufacturer.

Fabrication of PDMS-coated cover slips for cell culture

20 µL of UV curable resin was drop-casted onto 13 mm cover slips and allowed to spread for 10 min. The coated cover slips were then irradiated for 2 min by UV light in an oxygen-reduced atmosphere.

Rheological Measurements

Rheological measurements were performed on a hybrid rheometer (DHR-3) from TA Instruments fitted with a UV accessory. The upper parallel plate and the bottom quartz window, which is to allow the transmittance of UV light, are both 20 mm in diameter. UV irradiation was generated with an Omnicure S1500 mercury lamp (λ 280-600nm) and introduced into the Rheometer UV chamber via a flexible light guide. The intensity of the UV light was measured using a radiometer for calibration and controlled by the advanced TRIOS software during experiments.

Oscillations were set to controlled strain mode at 1 % strain, which was found to be within the linear viscoelastic region determined from initial amplitude sweeps. The UV-curable resin was sandwiched between two plates of the rheometer at a fixed gap of 250 µm while the axial force was controlled with a deviation of less than 0.1 N during the measurement. For *in-situ* monitoring of the progression of cross-linking, a time sweep (5 min in total) with fast sampling mode of 25 Hz to allow monitoring of the rapid rates of reaction. After 30s of equilibrium without UV exposure, the resin was irradiated for 2 min at the required intensity and the UV light was turned off for the remaining part of the experiment. Frequency sweep measurements were conducted before and after the UV cure to examine the change in rheological behaviour. All experiments were repeated in triplicate for each composition or condition.

Tensile mechanical characterisation

Tensile properties were determined for samples with different cross-linker chain lengths using an Instron frame equipped with a 5 N load cell. Rectangular samples with thickness of 3 mm (precise thicknesses were determined with a calliper) were used and measurements were carried out in triplicate. The measurement was conducted at room temperature at a constant strain rate of 1 mm/mm/minute. The initial region of low extension (0-10%) in the stress-strain plot was used to determine the tensile properties of samples.

Keratinocyte cells line culture and seeding onto substrates

Human keratinocyte HaCaT cells (Blizard Institute) were cultured in DMEM containing 10 % fetal bovine serum (FBS, PAA Laboratories), 1 % L-Glutamine (200 mM, Gibco) and 1% Penicillin-Streptomycin (5,000 U/mL, Gibco). HaCaT cells were harvested with trypsin (0.25 %) and Versene solution (0.2 g/L EDTA (Na4) in Phosphate Buffered Saline (Gibco)) and seeded onto PDMS substrates (functionalised with collagen I, in a 24-well plate) at a density of 20,000 per well (10,500 cell/cm^2). Cells were left to adhere and grow for 24 h in an incubator (37 °C and 5 % CO_2).

Fluorescence staining and microscopy

Keratinocyte HaCaT cells on PDMS were fixed with 4 % PFA (Sigma) for 10 min and permeabilized with 0.2 % Triton-X100 (Sigma) for 5 min at room temperature. Then substrates were incubated with Tetramethyl rhodamine isothiocyanate-phalloidin and DAPI in the blocking solution (10 % fetal bovine serum plus 0.25 % gelatine) for 1 h. Samples were mounted on glass slides with Mowiol reagent (Sigma). Images were acquired with a Leica DMI4000 fluorescence microscopy.

Live/Dead cell viability

The viability of HaCaT cells on PDMS was determined using a Live/Dead viability/cytotoxicity assay kit. In brief, HaCaT cells on PDMS were incubated in serum free DMEM with 2 µM Calcein AM and 4 µM ethidium homodimer-1 for 30 min (Gibco). After rinsing again with serum free DMEM, stained cells were imaged using a Leica DMI4000 fluorescence microscopy. The percentage of viable cells was calculated by counting the number of green (live) cells and dividing by the total number of cells including red (dead) cells.

Bonding of thiol-ene cross-linked PDMS to glass substrate

Prior to the bonding test, the UV curable resin was casted onto a conventional silicone master in a plastic petri dish and irradiated with UV light to pattern the surface of PDMS substrate. The PDMS samples were then cut in a size of 5 mm x 3 mm (patterned area) and 10 mm thick in order to be clamped onto the tensile kit combined to the SEM. Since there is no photoinitiator available in the already cross-linked material, a thin layer of photoinitator in diluted solution was applied on the PDMS sample and allowed to dry quickly in air. Then, the patterned PDMS substrate was aligned and brought into contact with a functionalised glass slide. This glass slide was pre-treated with 3-(trimethoxysilyl)propyl acrylate in toluene overnight prior to the bonding step. Samples were irradiated with UV light for 2 min to bond the two substrates.

***In-situ* recording of the adhesive failure with Scanning Electron Microscopy (SEM)**

The samples were tested using a Deben MICROTEST 200N tensile test rig combined with an FEI Quanta 3D ESEM. The setup of such system can be found in Fig. S1, Supplementary Information. Tensile tests were performed at a rate of 1 mm/min in situ with SEM microscopy. The adhesive failure of the PDMS sample from the functionalised glass coverslip was monitored and recorded with SEM microscopy (under high vacuum), along with the force-displacement data.

Results and discussion

In-situ rheological measurements during UV curing

We first investigated the cross-linking of high molecular weight PDMS via UV-initiated thiol-ene chemistry using commercially available telechelic vinyl-functionalised PDMS and thiol copolymer PDMS, as depicted in Fig. 1. The photoinitiator DMPA was employed to initiate this reaction at ambient temperature due to its high efficiency for the generation of reactive radicals [14]. To gain further insight into the kinetics of the crosslinking process, we used photo-rheology to monitor *in-situ* the evolution of dynamic rheological properties of the networks being formed via photo-induced cross-linking.

Fig. 2 shows a typical *in-situ* rheological profile acquired during the crosslinking of a resin formulated with ene:thiol ratio of 1:2 and a telechelic PDMS-vinyl of 1,000 cSt under a UV irradiation intensity of 94 mW/cm^2. The evolution of the elastic (G') and viscous (G") moduli during UV curing indicates the build-up of a microstructure as a result of the formation of thioether cross-links. As expected, before exposure to UV light (the first 30 s), the viscous modulus prevailed over the elastic component, indicating that the material is in a viscous sol state. Upon exposure to UV-light, both elastic and viscous moduli rapidly increased, with the elastic modulus progressing at a faster rate and eventually crossing over the loss modulus after 1.2 s. This cross-over point can be used as an approximation of the gelation point, at which either the weight average molecular weight diverges to infinity or one of the molecules has grown extremely large and its dimension is comparable to that of the macroscopic sample[32]. However, it should be noted that a true definition of the gelation point is that the tanδ becomes independent of the frequency at which shear is applied[33], but that monitoring such behaviour cannot be carried out fast enough to characterise the kinetics of the fast curing presently studied. Beyond this point, the network moduli continued to increase steadily with increasing cross-link density until the system reaches completion of the chemical reaction as shown as a plateau in the rheological profile. Over the course of gelation, the storage modulus, G', is seen to increase by approximately 3 orders of magnitude, showing a significant change in the mechanical properties of the cured material as a result of its transformation from a viscous liquid to a highly cross-linked network. Interestingly, the moduli reached a plateau within 2.5 s and the presence of oxygen in the system.

Importantly, the rate of sampling in our *in situ* rheological measurements, despite the high speed of the thiol-ene process and associated cross-linking, allowed the precise determination of the crossover between storage and loss moduli, which can be used as an approximation of the gelation point. Our results highlight the particularly fast curing rate of PDMS resins cross-linked via a UV-initiated thiol-ene process, despite the relatively high molecular weight (28,000 – 140,000 g/mol) of the siloxane precursors used. Muller et al.[18] and van de Berg et al.[20] reported the high efficiency of the cross-linking of silicones of moderate molecular weight (approximately 6,000g/mol), and followed the depletion of reactants (double bonds or thiol groups) using IR, Raman and NMR. Muller and Kunz found that the fully cross-linked network of formulations using vinyl-ene PDMS was only achieved after 2 min of UV curing while a fixed UV irradiation time (5 min) was used in the study of van de Berg et al. Similarly, thiol-ene chemistry was used to induce the gelation of various non-silicone based systems, for example, Crammer's work on the thiol-ene reaction between pentaerythritol tetrakis(2-mercaptoacetate) and different enes (diallyl, triallyl, dinorbonene and divinyl ether)[34] showing the highest conversions were attained between 2-8 min. Other studies suggests relatively slower curing rate including trimethylolpropane tris(2-mercaptoacetate) with trimethylolpropane dially ether (gelation time of 20 min)[35]; triallyl isocyanurate witth trimethylolpropane tris(2-mercaptoacetate) (gelation time of 36 min)[36], or with pentaerythritol tetrakis(2-mercaptoacetate) (gelation time of 5 min)[36]. Chambon and Winter also monitored the gelation PDMS networks by hydrosilation reactions using rheology and reported reaction times of 20 min[33]. Taken aside differences in experimental conditions between these different studies, such as the UV sources, irradiation intensity, chemistry and initiator type, the gelation time achieved in the present study is considerably faster than what was achieved using other strategies for the crosslinking of silicone elastomers. This difference is thought to result from the rate of the thiol-ene coupling (based on radical reactions, but less sensitive to oxygen and other quenching species than conventional free radical polymerisation of methacrylates or styrenic monomers) and the combination of a high functionality number PDMS-thiol (MW 4000-7000 g/mol; mercaptopropyl siloxane unit content is 100%) with high molecular weight telechelic alkene PDMS. The low T_g of silicones may also contribute to the fast reactivity of the present system by favouring the diffusion of reactive species.

The impact of alkene-thiol ratio

In order to investigate parameters impacting the gelation process as well as ultimate mechanical properties of the networks formed, the influence of the ratio of functional groups between alkene and thiol functions was studied. Specifically, we monitored the effect of the alkene-thiol ratio on the kinetics of the cross-linking reaction as well as the shear storage and loss moduli. A series of UV curable resins was prepared by using a fixed concentration of photoinitiator (thiol : photoinitiator = 1 : 0.1 molar ratio, c.a. 0.2 wt%) and UV irradiation (94 mW/cm^2) with the PDMS-vinyl of 1,000 cSt while varying the alkene to thiol ratio from 1:1 up to 1:3. As can be seen in Fig. 3, all formulations tested start with similar storage moduli (approximately 0.1 Pa) prior to UV curing, but exhibit distinct moduli after the completion of the curing. Fig. 3D indicates that the storage modulus was maximum (67 kPa) with a ratio of 1:2, whereas the 1:1 ratio resulted in the lowest storage modulus (5 kPa). Hence the maximum storage modulus of the final cross-linked network does not occur at a balanced stoichiometry but instead at stoichiometric ratios higher than unity, displaying an excess of thiol residues. In

contrast to the theory that perfect networks are obtained at a stoichiometric ratio of 1:1[18, 20, 33], these results imply that the networks formed display defects, perhaps via incomplete reaction of all alkene end chains. Looping defects only are unlikely to explain such differences as they should not be as dependent on the ratios of the two functional groups. A control experiment carried out in the absence of vinyl terminated PDMS confirmed that cross-linking does not occur (no change in moduli observed). However, carbon radical recombinations, which have been previously identified as a primary termination mechanism in thiol-ene based polymer-polymer coupling[37, 38], may account for the off stoichiometry optimum observed. Indeed, a slight decrease in alkene concentration may favour transfer to thiols and improve efficient crosslinking of the network.

Such imperfection in the networks formed are also evidenced by frequency sweep data, shown in Fig. 3C. The networks formed from the alkene:thiol ratios of 1:1 and 1:3 respond more strongly to changes in the oscillation frequency than the others, indicating a stronger viscous component. This would be aligned with the concept that, at low thiol content (1:1), some alkene-terminated chains do not contribute to the cross-linking, leading to an increased number of dangling or looping segments, and consequently acting as network plasticizers. In contrast, at high thiol content (1:3), the excess of PDMS-thiol should result in fewer cross-links per chain and therefore displays a decreased storage modulus. This phenomenon was also noted by Muller et al[18] for thiol-ene crosslinked silicones, reporting that the network density increased with increasing thiol content and achieved optimum values in the range of balanced stoichiometric before starting to decrease beyond that point.

The ratio of reactive groups had a strong impact on the gelation time observed during photo-rheology experiments (Fig. 3B). Since the chain transfer, where the carbon-centered radical is transferred to another thiol functional group, is a key step in the thiol-ene reaction mechanism, the thiol content must influence the efficiency of hydrogen-abstraction and as a result the rate at which gelation is reached. The plot in Fig. 3B presents the gelation time as a function of thiol content. Generally, the gelation can be achieved faster with increasing thiol content, but remains almost constant beyond a ratio of 1:2. These observations are well aligned with literature reports that suggested that the favoured recombination of thiyl radicals in conditions with a large excess of thiol could account for such behaviour[18], although we did not see any evidence for this in control experiments carried out in the absence of vinyl-terminated macromonomers (not shown). However, the changes in relative concentrations of alkenes and thiols would also be expected to alter gelation kinetics in simple mathematical models (see below). The decrease in lag time before the moduli starts increasing (shorter lag times for lower ratios of alkenes) may also indicate a higher sensitivity of the forming network to oxygen or alkyl radical recombintations in conditions for which thiols are not in excess.

The impact of UV irradiation

As the photoinitiator is activated by UV light, it is important to explore the role of the UV intensity on the initiation of the cross-linking process. The effect of irradiation intensity (5, 10, 50 and 94 mW/cm^2) was studied using the resins formulated from PDMS-vinyl of 1,000cSt and the ratio of ene to thiol was 1:2. Fig. 4 indicates a strong dependence of cross-linking rates on the UV intensity, whereas the storage modulus only shows a slight decrease with decreasing intensities. The gelation time significantly drops from 21.5 ± 0.4 s at 5 mW/cm^2 to 1.24 ± 0.03 s at 94 mW/cm^2, as a result of the larger number of photoinitiators excited at higher UV light intensities and associated increase in the formation of free radicals, leading to a faster gelation. The slight decrease of storage modulus at lower intensities could be attributted to defects present in the network and the potential quenching of some radicals by oxygen species.

The evolution of the storage modulus G' with irradiation time also revealed a lagging period after exposures of the systems to UV light, which increased with decreasing light intensities. The lagging period might be a result of the initial slow increase in viscosity of the system, considering the step growth mechanism of the reaction, but may also be associated with the retardation of oxygen dissolved in silicone materials. In general, conventional radical reactions are strongly influenced by the presence of oxygen either in the surrounding environment or freely soluble in the reactants. Oxygen reacts with an alkyl radicals to form peroxy radicals, resulting in the termination of the reaction. Thiol-ene reactions, on the other hand, are less susceptible to such effects as a result of the fast transfer to thiyl radicals and the regeneration of thiyl radicals via hydrogen-abstraction from peroxy radicals[39]. Such effects might also be facilitated by the high permeability and diffusion constant of oxygen in silicone derivatives [40]. As seen in Fig. 4A, this effect can be diminished by increasing the intensity of UV light, which leads to a faster consumption of oxygen present in the system. This observation is similar to previous reports showing that the polymerisation reaction starts once the concentration of oxygen is sufficiently low [18]. The log-log relationship observed between the gelation time and the intensity of the light used, in agreement with Eq 10, indicates that such oxygen inhibition is hidden within the efficiency terms of the initiation step (Eq 1). Hence, based on our observations, the removal of air is not necessary for the curing of thiol-ene silicones, however an atmosphere presenting a reduced level of oxygen would result in better and faster curing on the surface of the corresponding resins.

The impact of cross-linker chain length

The viscosity of a mixture plays an important role in the design of a formulation for a specific application. This may in turn influence the mechanical properties of the final networks. The impact of the viscosity of the siloxane system on thiol-ene cross-linking kinetics and the final mechanical behaviour of the networks formed were studied next. In this study, we varied the chain lengths of the telechelic vinyl-functionalised PDMS

(M_w between 6,000 and 140,000 g/mol, corresponding to changes in the viscosity of this macromonomer in the range of 1,000 - 100,000 cSt) whilst keeping the ene to thiol ratio constant at 1:2. The experiments were carried out under constant UV irradiation of 94 mW/cm^2.

Fig. 5A shows typical time sweeps for the evolution of the storage modulus of the mixtures as a function of time, for different viscosities of macromonomers (irradiation was switched on at 30 s). With a molecular weight of 5,500 g/mol for PDMS-thiol 100, whilst telechelic vinyl-PDMS had molecular weights varying from 6,000 to 140,000 g/mol, the amount (weight or volume fraction) of the multifunctional PDMS-thiol 100 in the resin is very low, allowing to approximate the viscosity of the starting reaction mixture to that of the vinyl-terminated PDMS. Fig. 5B shows that the gelation time increases linearly in a log-log scale with increasing viscosity of the cross-linker. Such trend clearly highlights the importance of molecular diffusion as a key factor controlling the rate of thiol-ene reactions in the present silicone materials. We developed a simple mathematical model accounting for the kinetics observed.

The rate of photochemical initiation R_i is defined by the quantum yield of the initiation Φ, the concentration of photoinitiator [I], the intensity of incident UV light I_0 and the extinction coefficient of the initiator (per unit of length of the sample) ε in a simplified relationship[41]

$$R_i = 2\,\Phi\,I_0\,\varepsilon\,[I] \qquad \textbf{Eq 1}$$

Thus, for cases where the type of photoinitiator and concentrations are the same, as in this experiment, along with a fixed gap between the two plates of the rheometer, the initiation rate must be directly proportional to the intensity of UV incident light.

Using this simple relationship to describe the rate of photoinitiation, we propose a simple kinetic model that correlates the gelation time with reaction parameters. In this model, we make the assumption that the main termination mechanism is via carbon radical bimolecular recombination (see Scheme 1), which was previously proposed as the main termination mechanism for thiol-ene reactions previously[37, 38]. Termination by transfer of radicals to oxygen was neglected at the high light intensities used. The following equations describe the rates of changes in concentration of the different radical species:

$$\frac{d([C^\bullet])}{dt} = k_p[RS^\bullet][C{=}C] - k_{ct}[C^\bullet][RSH] - k_t[C^\bullet]^2 \qquad \textbf{Eq 2}$$

$$\frac{d([RS^\bullet])}{dt} = k_i[I^\bullet][RSH] - k_p[RS^\bullet][C=C] + k_{ct}[C^\bullet][RSH] \qquad \textbf{Eq 3}$$

$$\frac{d([I^\bullet])}{dt} = 2\,\Phi\,I_0\,\varepsilon\,[I] - k_i[I^\bullet][RSH] \qquad \textbf{Eq 4}$$

in which $[C=C]$, $[RSH]$, $[I]$, $[C^\bullet]$, $[RS^\bullet]$ and $[I^\bullet]$ are the concentrations of double bonds, thiol groups, initiator, carbon radical, thiyl radical and photo-cleaved initiating species, respectively. Assuming that a steady-state is quickly reached for which the rates of formation of photo-cleaved initiators and disappearance of carbon radicals are balanced and for which the concentration of thiyl radicals remains stable, we can write:

$$\frac{d([I^\bullet])}{dt} = -\frac{d([C^\bullet])}{dt} \quad \textbf{Eq 5} \quad \text{and} \quad \frac{d([RS^\bullet])}{dt} = 0 \quad \textbf{Eq 6}$$

The rate of formation of crosslinks is then given by the following equation:

$$\frac{d([X])}{dt} = k_{ct}[C^\bullet][RSH] = \frac{k_{ct}}{k_t^{1/2}}\,(2\,\Phi\,I_0\,\varepsilon\,[I])^{1/2}[RSH] \qquad \textbf{Eq 7}$$

where [*X*] is the concentration of crosslinks formed, assuming that the chain transfer step is the one generating effective crosslinks. After integration and extracting the viscosity of the medium η from rate constants, we obtain:

$$[X]_c = \frac{k'_{ct}}{k'^{1/2}_t}\left(\frac{2\,\Phi\,I_0\,\varepsilon\,[I]_0}{\eta}\right)^{1/2}[RSH]_0 t_c \qquad \textbf{Eq 8}$$

where $[RSH]_0$ and $[I]_0$ are the initial concentrations in thiol functions and initiator, respectively, and t_c and $[X]_c$ are the time at the gelation point and corresponding concentration, respectively. In addition, rate constants are inversely correlated to the viscosity of the system η via the following equations[42]

$$k_{ct} = \frac{k'_{ct}}{\eta}\,; \qquad k_t = \frac{k'_t}{\eta} \qquad \textbf{Eq 9}$$

where k_{ct}' and k_t' are the reduced rate constants of chain transfer and termination, respectively. Finally, we obtain the following log/log relationship:

$$\log(t_c) = \log(k_{app}) + \log\left(\frac{[X]_c}{[RSH]_0 {I_0}^{1/2}{[I]_0}^{1/2}}\right) + \frac{1}{2}\log(\eta) \qquad \textbf{Eq 10}$$

where k_{app} is an apparent rate constant for this system.

$$k_{app} = \frac{k'^{1/2}_t}{k'_{ct}(2\,\Phi\,\varepsilon)^{1/2}} \qquad \textbf{Eq 11}$$

The extent of reaction for which gelation should occur in this system can be predicted from Flory-Stockmayer equation[41], which allows the determination of the apparent rate constant of cross-linking from Equation **10**. In our system, we calculated a gelation point of 11%, calculated $[X]_c$ from this value and extracted from the kinetics plot a k_{app} of 6.6 ± 1.1 $m^{1/2}mol^{1/2}L^{-1/2}$. The relatively good agreement between the slope predicted and that measured (0.5 from Eq 10 and 0.20 ± 0.03 from our results) confirms the validity of this simple model to capture important kinetics parameters controlling the formation of silicone networks via thiol-ene chemistry and in particular the dependence of such kinetics on the viscosity of the system.

Despite the wide range of molecular weights between the different vinyl telechelic crosslinkers used, all moduli obtained after UV curing were relatively comparable, in the range of 70 to 120 kPa (Fig. 5D). This contrast with the initial broad range of viscosities and associated storage moduli of uncured resins, which varied from 0.01 to 100 Pa. Fig. 6A shows the comparison of the evolution of storage modulus obtained by rheology and that of the Young's modulus from tensile

mechanical testing with increasing viscosity of cross-linker. The Mooney-Rivlin equation[43] was used to calculate the cross-link density from tensile measurements and the relationship measured between cross-link density and viscosity of cross-linkers is presented in Fig. 6B. This trend slightly differs from the trend in moduli, indicating the importance of entanglement in determining the mechanical behaviour of these silicone materials, in particular for the highest molecular weight crosslinkers. The data obtained from frequency sweeps (Fig. 5C) also suggest a higher viscous component and imperfection of the networks generated from high molecular weight cross-linkers. The low moduli and degree of cross-link density measured for the shortest crosslinker implies an increased number of defects. This could be the result from increased intramolecular cyclization due to low molecular weight side-chains, yielding to the formation of loops within the macromolecule network that do not contribute to crosslinks or bulk mechanics[44].

Cytocompatibility

Due to the importance of silicone based biomaterials for a range of biomedical applications[45, 46], we investigated next the cytocompatibility of the materials generated. An interesting feature of the thiol-ene silicones presently reported is the ability to control their mechanical properties (through the thiol-ene ratio) and biofunctionalisation (through remaining reactive thiols). Substrates with high (126kPa) and low (5kPa) storage moduli were used to culture HaCaT cells. A live/dead assay was used to quantify cytocompatibility (Fig. 7A) and showed that both stiffnesses of PDMS substrates did not significantly affect cell survival relative to the plastic controls. A slight decrease in viability was measured for softer substrates that had not been coated with collagen, presumably as a result of reduced adhesion in the absence of intergrin ligands. Indeed, cell densities were lower in substrates that had not been conditioned through incubation in a collagen solution. The low stiffness substrates were fabricated using an ene-to-thiol ratio of 1:1 as compared to the 1:2 ratio for the stiff samples. This excess of thiol content may impact the adhesion of proteins from the medium and subsequently alter cell adhesion. In addition, immunostaining gave clear evidence that cell adhesion to these PDMS substrates was allowing the assembly of a mature cytoskeleton, with structured stress fibres (Fig. 7B). This implies that the formation of focal adhesions is allowed on silicone substrates with the range of stiffnesses probed, similarly to our previous report using conventional silicones[47]. Hence thiol-ene PDMS appears as a useful biomaterial for the culture of cells on substrates with controlled bulk mechanical properties.

Adhesion to glass substrate

Microfluidic systems are at the centre of a number of applications in the biomedical field, for example for the development of novel assays for drug testing, biosensing[48, 49] or the mimicking of higher level structure and function of tissues[50-52]. In such systems, PDMS is the material of choice as it allows the simple microfabrication of microchannels[46] via replication from masters generated through conventional photolithography protocols. However, this requires sealing devices (and channels) by bonding the patterned PDMS substrate to a flat platform, usually glass. Several bonding strategies have been reported[46, 53-57] but oxygen plasma treatment and thermocurring are still the most common techniques. However, these treatments can damage pre-biofunctionalized surfaces and do not always result in strong bonding, leading to leakage of the device. In addition, further functionalisation of the PDMS channels require further chemical modification. To assess the feasibility of using the thiol-ene system developed in this study in promoting the bonding between a patterned PDMS sample and a glass substrate, the resin formulated with alkene:thiol ratio of 1:2 and vinyl-PDMS of 10,000 cSt was cast onto a conventional master and exposed to UV light for curing. The cured substrate was then easily peeled off from the master. SEM images of such patterned surface are gathered in Fig. 8A, confirming that the quality of the pattern is preserved during this step.

An in situ tensile test whilst imaging with an SEM indicated excellent adhesive properties of such system with failure mainly occurring from bulk of the silicone rather than detachment at the interface (see Supplementary Fig. S1 and Supplementary Video). As can be seen from the recoded video, the PDMS resin is subjected to significant stress and elongates prior to cohesive failure. Such bulk failure is also confirmed via examination of the resulting surfaces (after fracture) via SEM (Fig. 8C, 8D). Clear residues are observed on the glass substrates and the pattern of the silicone sample is clearly disrupted. To compare this system with current methods used for the fabrication of microfluidic devices from silicone materials, we carried out the same experiment with the well-known Sylgard 184. The Sylgard 184 mixture (mixing ratio of 10:1 between the base and the curing agent) was cured at 60^{o}C for 3 h and bonded to the glass slide, after oxygen plasma treatment, whilst applying a slight pressure. The bonded structure typically failed during the attachment into the tensile kit in the SEM chamber, highlighting a weaker adhesion compared to thiol-ene bonding. In addition, the surface of the PDMS sample bonded with plasma, after detachment, appeared relatively intact, indicating adhesive failure at the interface. Thus, the use of UV curing of thiol-ene PDMS to bond with alkene functionalised interfaces appears to be a promising approach for constructing microfluidic systems.

Conclusions

We have utilised an *in-situ* technique to investigate the evolution of rheological properties of UV cross-linked silicone materials via thiol-ene chemistry and macroscopic properties such as storage modulus and gelation time. The impact of different factors (functional equivalent between thiol- and ene- groups, cross-linker chain length and UV irradiation intensity) on the gelation behaviour and mechanical properties has been investigated. The gelation was found to occur extremely fast, even in the presence of oxygen in the system

and was found to be diffusion controlled, regulated by the viscosity of the silicones used. Interestingly, little variation was observed for the storage modulus of cross-linked networks generated from macromonomers with varying viscosities or at different UV light intensities. However, the mechanical properties of these silicones was effectively controlled by the ratio of thiol-to-ene moieties. Therefore such silicones may find useful applications in conditions for which fast cure rates in mild conditions are required. In addition, the ability to preserve good mechanical properties, when starting from monomer mixtures with a wide range of viscosities is interesting for 3D printing and microfabrication applications. Finally, the good cytocompatibility of the resulting thiol-ene PDMS networks was demonstrated for HaCaT cells and highlighted the potential of such biomaterials for biomedical applications and cell culture. In particular, the ability to systematically vary the mechanical properties of these substrates whilst allowing their biofunctionalisation with cell adhesive molecules (potentially also via thiol-ene radical chemistry or via Michael addition) is attractive to study further mechanobiology and to improve long term stem cell culture.

Acknowledgements

K.D.Q.N. thanks FormFormForm Ltd. for a studentship. W.M. thanks the Engineering and Physical Sciences Research Council (EP/L505602/1) for a case studentship.

References

1. D. T. Liles, *The Fascinating World of Silicones*, 2012.
2. J. E. Mark, H. R. Allcock and R. West, in *Inorganic polymers*, Oxford University Press, 2005, pp. 154-199.
3. A. Colas and J. Curtis, in *Biomaterials science : an introduction to materials in medicine*, ed. B. D. Ratner, 2004.
4. J. F. Zhang, Y. Chen and M. A. Brook, *Langmuir*, 2013, **29**, 12432-12442.
5. J. M. Anderson, N. P. Ziats, A. Azeez, M. R. Brunstedt, S. Stack and T. L. Bonfield, *Journal of Biomaterials Science, Polymer Edition*, 1996, **7**, 159-169.
6. M. Li, K. G. Neoh, L. Q. Xu, R. Wang, E.-T. Kang, T. Lau, D. P. Olszyna and E. Chiong, *Langmuir*, 2012, **28**, 16408-16422.
7. A. S. Mikhail, J. J. Ranger, L. Liu, R. Longenecker, D. B. Thompson, H. D. Sheardown and M. A. Brook, *Journal of biomaterials science. Polymer edition*, 2010, **21**, 821-842.
8. F. Abbasi, H. Mirzadeh and A.-A. Katbab, *Polymer International*, 2001, **50**, 1279-1287.
9. J. Roth, V. Albrecht, M. Nitschke, C. Bellmann, F. Simon, S. Zschoche, S. Michel, C. Luhmann, K. Grundke and B. Voit, *Langmuir*, 2008, **24**, 12603-12611.
10. F. Sarvi, Z. Yue, K. Hourigan, M. C. Thompson and P. P. Y. Chan, *Journal of Materials Chemistry B*, 2013, **1**, 987-996.
11. A. M. Ferreira, I. Carmagnola, V. Chiono, P. Gentile, L. Fracchia, C. Ceresa, G. Georgiev and G. Ciardelli, *Surface and Coatings Technology*, 2013, **223**, 92-97.
12. *Journal*.
13. C. E. Hoyle and C. N. Bowman, *Angewandte Chemie International Edition*, 2010, **49**, 1540-1573.
14. C. E. Hoyle, T. Y. Lee and T. Roper, *Journal of Polymer Science Part A: Polymer Chemistry*, 2004, **42**, 5301-5338.
15. A. Dondoni, *Angewandte Chemie International Edition*, 2008, **47**, 8995-8997.
16. S. Di Cio and J. E. Gautrot, *Acta Biomaterialia*, 2016, **30**, 26-48.
17. K. Y. Tan, M. Ramstedt, B. Colak, W. T. S. Huck and J. E. Gautrot, *Polymer Chemistry*, 2016, **7**, 979-990.
18. U. Muller, A. Kunze, C. Herzig and J. Weis, *J. Macromol. Sci.-Pure Appl. Chem.*, 1996, **A33**, 439-457.
19. C. Decker and T. N. T. Viet, *Polymer*, 2000, **41**, 3905-3912.
20. O. van den Berg, L.-T. T. Nguyen, R. F. A. Teixeira, F. Goethals, C. Özdilek, S. Berghmans and F. E. Du Prez, *Macromolecules*, 2014, **47**, 1292-1300.
21. L. Xue, Y. Y. Zhang, Y. J. Zuo, S. Diao, J. Zhang and S. Y. Feng, *Materials Letters*, 2013, **106**, 425-427.
22. Y. Zuo, H. Lu, L. Xue, X. Wang, L. Wu and S. Feng, *Chemistry – A European Journal*, 2014, **20**, 12924-12932.
23. M. M. Ozmen, Q. Fu, J. Kim and G. G. Qiao, *Chemical Communications*, 2015, **51**, 17479-17482.
24. R. F. A. Teixeira, O. van den Berg, L.-T. T. Nguyen, K. Fehér and F. E. Du Prez, *Macromolecules*, 2014, **47**, 8231-8237.
25. H. Yang, Q. Zhang, B. Lin, G. Fu, X. Zhang and L. Guo, *Journal of Polymer Science Part A: Polymer Chemistry*, 2012, **50**, 4182-4190.
26. H. Yang, M. Xu, L.-X. Guo, H.-F. Ji, J.-Y. Wang, B.-P. Lin, X.-Q. Zhang and Y. Sun, *RSC Adv.*, 2015, **5**, 7304-7310.
27. L. M. Campos, I. Meinel, R. G. Guino, M. Schierhorn, N. Gupta, G. D. Stucky and C. J. Hawker, *Advanced Materials*, 2008, **20**, 3728-3733.
28. L. M. Campos, T. T. Truong, D. E. Shim, M. D. Dimitriou, D. Shir, I. Meinel, J. A. Gerbec, H. T. Hahn, J. A. Rogers and C. J. Hawker, *Chemistry of Materials*, 2009, **21**, 5319-5326.
29. C. F. Carlborg, T. Haraldsson, K. Oberg, M. Malkoch and W. van der Wijngaart, *Lab on a Chip*, 2011, **11**, 3136-3147.
30. M. A. Cole and C. N. Bowman, *Journal of Polymer Science Part A: Polymer Chemistry*, 2013, **51**, 1749-1757.
31. K. Goswami, A. L. Skov and A. E. Daugaard, *Chemistry – A European Journal*, 2014, **20**, 9230-9233.
32. F. Chambon and H. H. Winter, *J Rheol*, 1987, **31**, 683-697.
33. H. H. Winter and F. Chambon, *Journal of Rheology (1978-present)*, 1986, **30**, 367-382.
34. N. B. Cramer and C. N. Bowman, *J. Polym. Sci. Pol. Chem.*, 2001, **39**, 3311-3319.
35. B.-S. Chiou and S. A. Khan, *Macromolecules*, 1997, **30**, 7322-7328.
36. B. S. Chiou, R. J. English and S. A. Khan, *Macromolecules*, 1996, **29**, 5368-5374.
37. S. K. Reddy, N. B. Cramer and C. N. Bowman, *Macromolecules*, 2006, **39**, 3673-3680.
38. S. P. S. Koo, M. M. Stamenović, R. A. Prasath, A. J. Inglis, F. E. Du Prez, C. Barner-Kowollik, W. Van Camp and T. Junkers, *Journal of Polymer Science Part A: Polymer Chemistry*, 2010, **48**, 1699-1713.
39. N. B. Cramer, J. P. Scott and C. N. Bowman, *Macromolecules*, 2002, **35**, 5361-5365.
40. J. E. Mark, *Accounts of Chemical Research*, 2004, **37**, 946-953.
41. G. G. Odian, Principles of polymerization).

42. D. L. Kurdikar and N. A. Peppas, *Macromolecules*, 1994, **27**, 4084-4092.
43. L. H. Sperling, *Introduction to physical polymer science*, Wiley, New York, 4th edn., 2006.
44. E. Saldívar-Guerra and E. Vivaldo-Lima, *Handbook of polymer synthesis, characterization, and processing*, 2013.
45. J. Curtis and A. Colas, in *Biomaterials science : an introduction to materials in medicine*, ed. B. D. Ratner, 2004.
46. J. C. McDonald and G. M. Whitesides, *Accounts of Chemical Research*, 2002, **35**, 491-499.
47. B. Trappmann, J. E. Gautrot, J. T. Connelly, D. G. T. Strange, Y. Li, M. L. Oyen, M. A. Cohen Stuart, H. Boehm, B. Li, V. Vogel, J. P. Spatz, F. M. Watt and W. T. S. Huck, *Nat Mater*, 2012, **11**, 642-649.
48. M. Rothbauer, D. Wartmann, V. Charwat and P. Ertl, *Biotechnology Advances*, 2015, **33**, 948-961.
49. D. Mark, S. Haeberle, G. Roth, F. von Stetten and R. Zengerle, *Chemical Society Reviews*, 2010, **39**, 1153-1182.
50. D. Huh, B. D. Matthews, A. Mammoto, M. Montoya-Zavala, H. Y. Hsin and D. E. Ingber, *Science*, 2010, **328**, 1662-1668.
51. D. Huh, Y.-s. Torisawa, G. A. Hamilton, H. J. Kim and D. E. Ingber, *Lab on a Chip*, 2012, **12**, 2156-2164.
52. S. N. Bhatia and D. E. Ingber, *Nat Biotech*, 2014, **32**, 760-772.
53. H. Wu, B. Huang and R. N. Zare, *Lab on a Chip*, 2005, **5**, 1393-1398.
54. C. S. Thompson and A. R. Abate, *Lab on a Chip*, 2013, **13**, 632-635.
55. J. F. Ashley, N. B. Cramer, R. H. Davis and C. N. Bowman, *Lab on a Chip*, 2011, **11**, 2772-2778.
56. F. Saharil, C. F. Carlborg, T. Haraldsson and W. van der Wijngaart, *Lab on a Chip*, 2012, **12**, 3032-3035.
57. T. M. Sikanen, J. P. Lafleur, M. E. Moilanen, G. S. Zhuang, T. G. Jensen and J. P. Kutter, *J. Micromech. Microeng.*, 2013, **23**, 7.

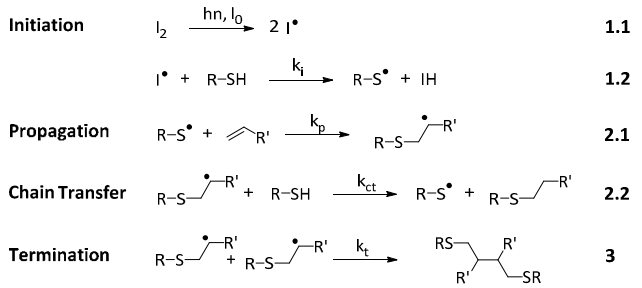

Scheme 1 Reaction mechanism for UV-initiated thiol-ene coupling

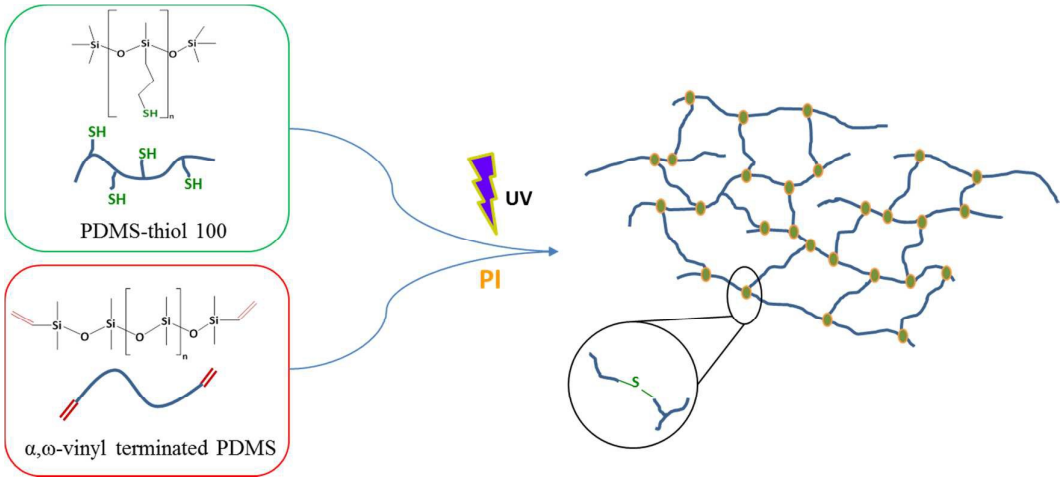

Fig. 1 Schematic representation of UV-induced thiol-ene cross-linking of PDMS-based material

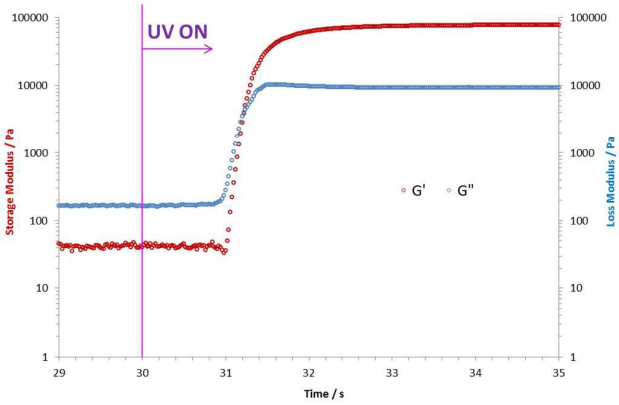

Fig. 2 Example of evolution of elastic (G') and viscous (G") moduli during UV curing obtained by using in-situ rheology. Here, the frequency and strain % of oscillation are 25 Hz and 1%, respectively. The sample was conditioned for 30s prior to UV exposure and irradiated for 120s. An inset in the region the cross-linking occurring shows a better illustration of gelation point.

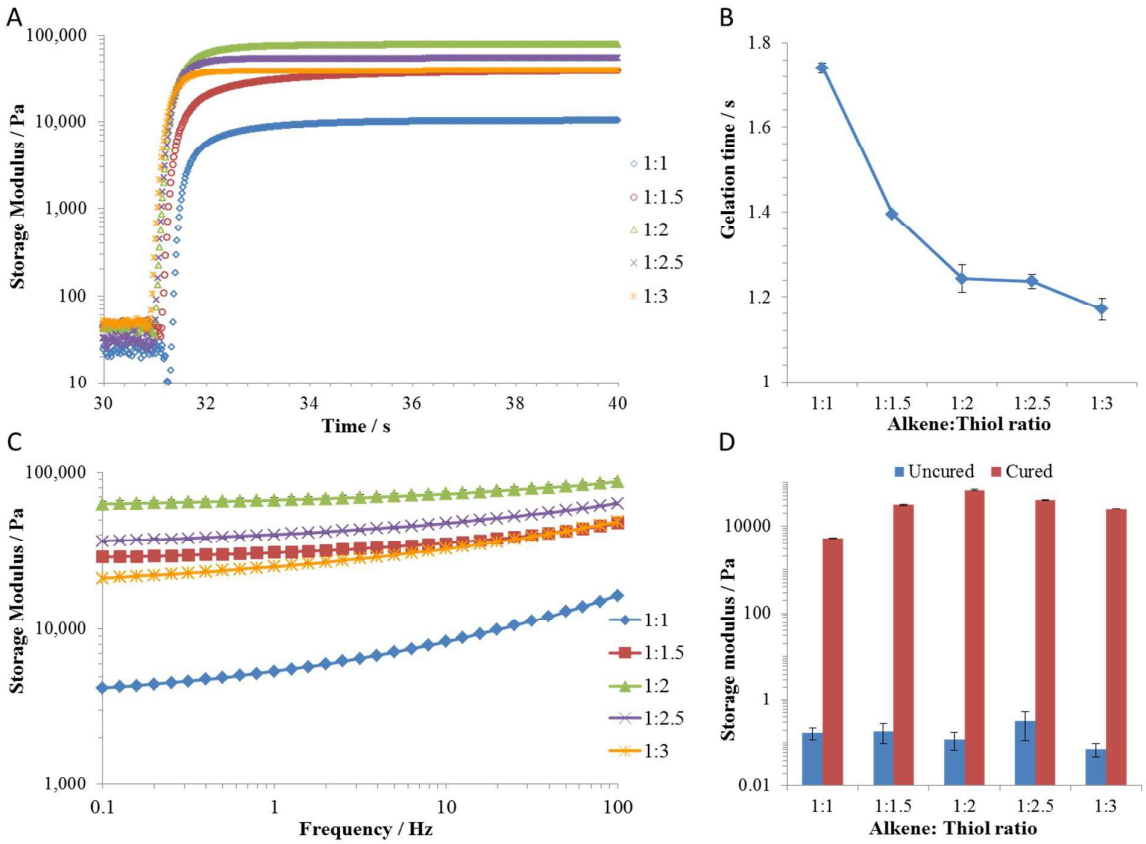

Fig. 3 Impact of alkene-to-thiol equivalent ratios on the gelation behaviour and the mechanical properties of cross-linked PDMS network via thiol-ene chemistry. A. Time sweep (oscillating amplitude of 1% strain at 25 Hz) shows the evolution of storage modulus (G') during UV irradiation (UV irradiated at 94 mW/cm^2). The UV curable resins were prepared from different alkene-to-thiol molar ratios (see legends), with cross-linker's viscosity of 1,000 cSt, and DMPA as photoinitiator (thiol:photoinitiator molar ratio of 1:0.1, c.a. 0.2 wt%). B. Gelation times were determined from the rheological profiles by *in-situ* rheology. C. Frequency sweeps (oscillation amplitude of 1% strain) were carried out for the characterisation of cross-linked PDMS. D. Comparison of storage modulus G' (at frequency of 1Hz obtained from frequency sweeps) of the resins before UV irradiation and the cross-linked silicones.

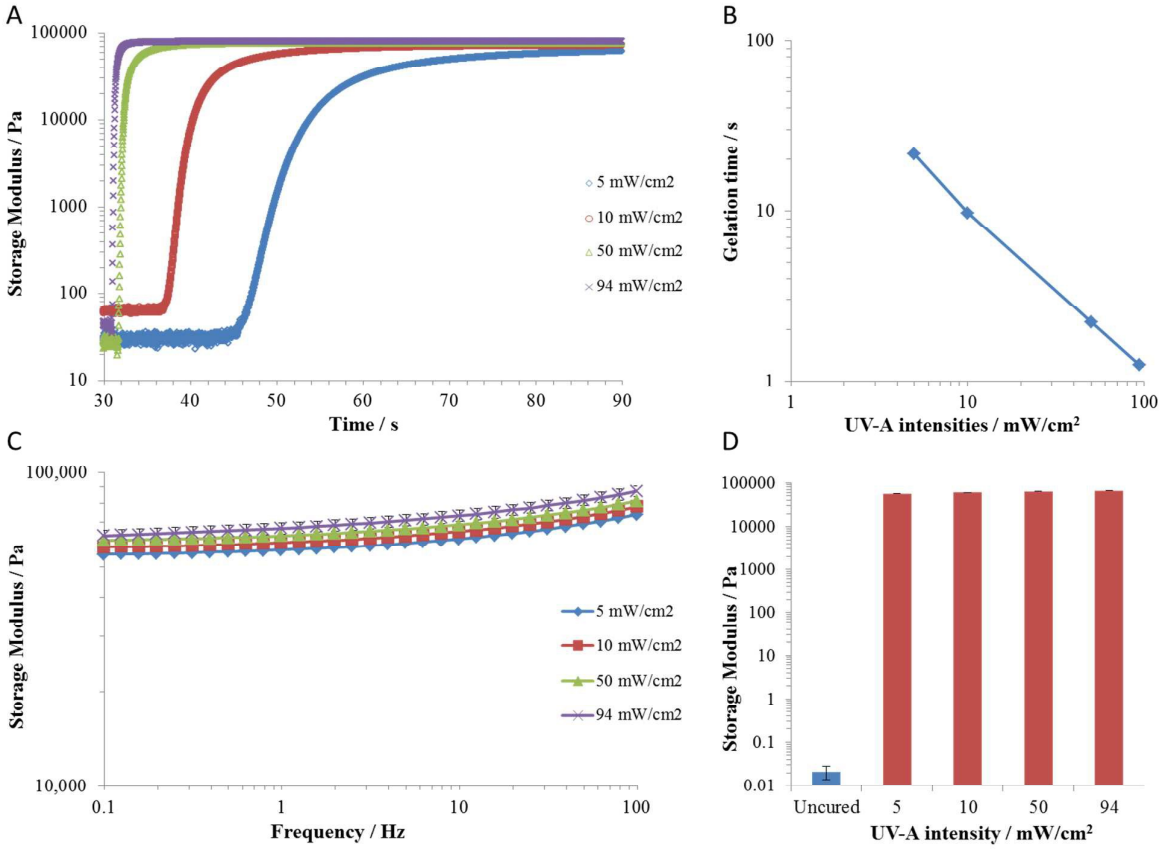

Fig. 4 Impact of UV irradiance on the gelation behaviour and the mechanical properties of cross-linked PDMS network via thiol-ene chemistry. A. Time sweep (oscillating amplitude of 1% strain at 25 Hz) shows the evolution of storage modulus (G') at different UV irradiance (see legend). The UV curable resin was prepared with alkene:thiol ratio of 1:2, cross-linker's viscosity of 1,000 cSt and DMPA as photoinitiator (thiol:photoinitiator molar ratio of 1:0.1). B. Gelation times were determined from the rheological profiles by *in-situ* rheology. C. Frequency sweeps (oscillation amplitude of 1% strain) were carried out for the characterisation of cross-linked PDMS. D. Comparison of storage modulus G' (at frequency of 1 Hz obtained from frequency sweeps) of the uncured resin and the cross-linked silicones at different UV intensities.

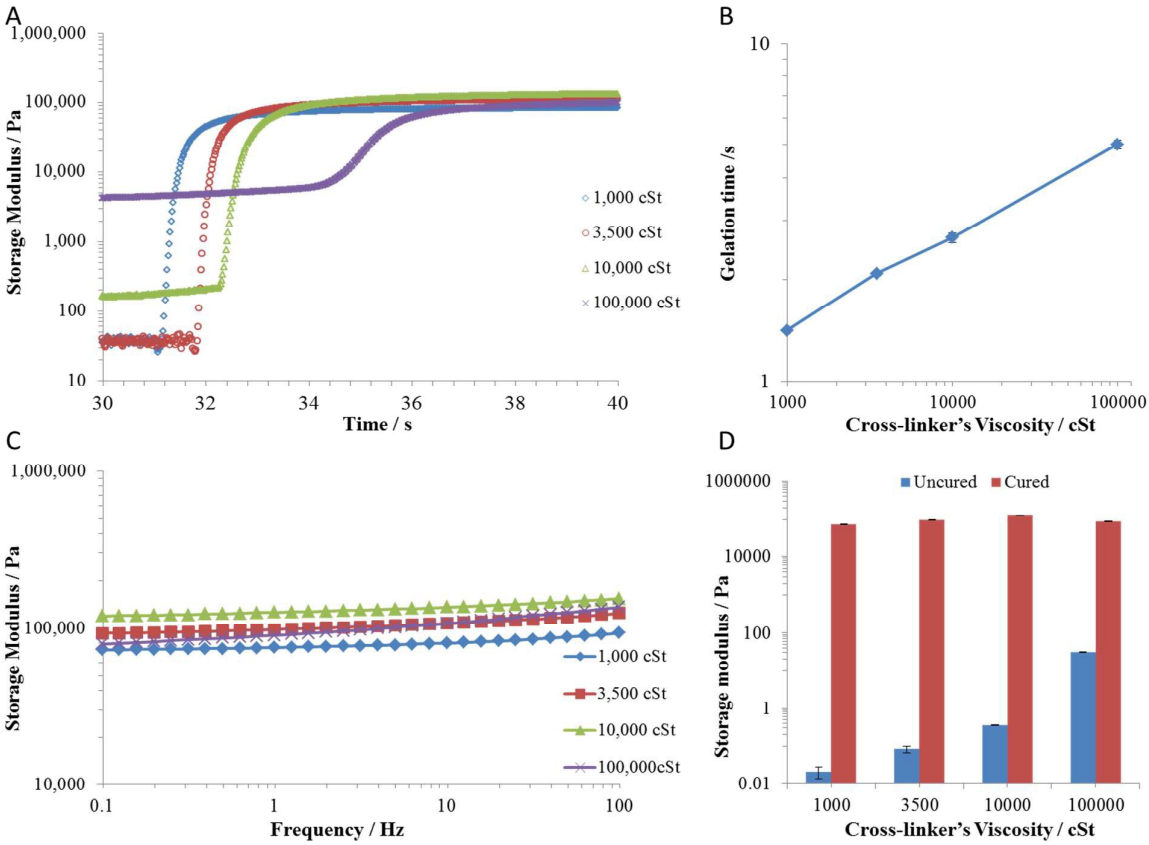

Fig. 5 Impact of cross-linker's viscosity on the gelation behaviour and the mechanical properties of cross-linked PDMS network via thiol-ene chemistry. A. Time sweep (oscillating amplitude of 1% strain at 25 Hz) shows the evolution of storage modulus (G') during UV irradiation (UV irradiated at 94 mW/cm^2). The UV curable resins were prepared from different viscosities of cross-linker (see legends), with alkene:thiol ratio of 1:2, and DMPA as photoinitiator (thiol:photoinitiator molar ratio of 1:0.1). B. Gelation times were determined from the rheological profiles by *in-situ* rheology. C. Frequency sweeps (oscillation amplitude of 1% strain) were carried out for the characterisation of cross-linked PDMS. D. Comparison of storage modulus G' (at frequency of 1 Hz obtained from frequency sweeps) of the resins before UV irradiation and the cross-linked silicones.

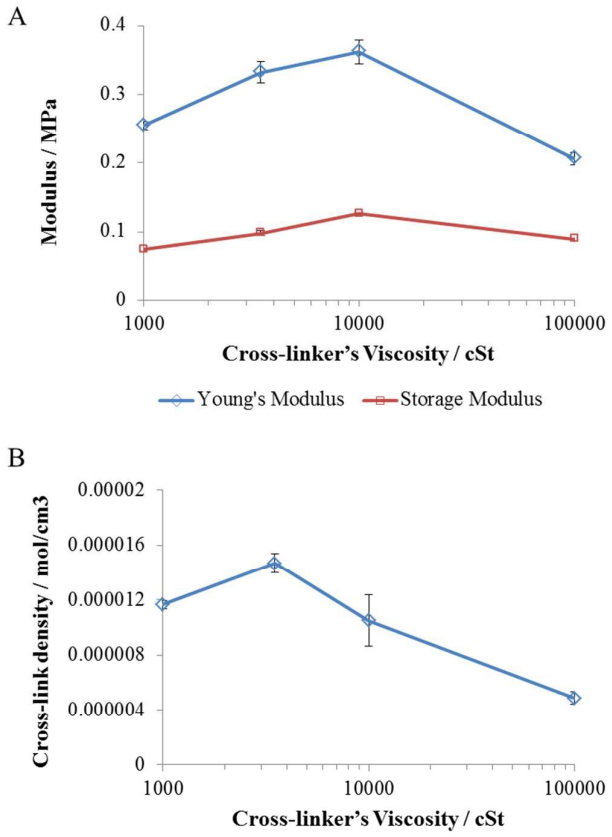

Fig. 6 A. Comparison between Young's Modulus, E, and Storage Modulus, G',with different viscosities of cross-linker (resins formulated with alkene:thiol equivalent ratio of 1:2 and thiol:DMPA molar ratio of 1:0.1) and (B) the cross-link densities calculated from tensile mechanical properties by mean of Mooney-Rivlin relation. Representative examples of the corresponding stress-strain curves can be seen in Figure S2.

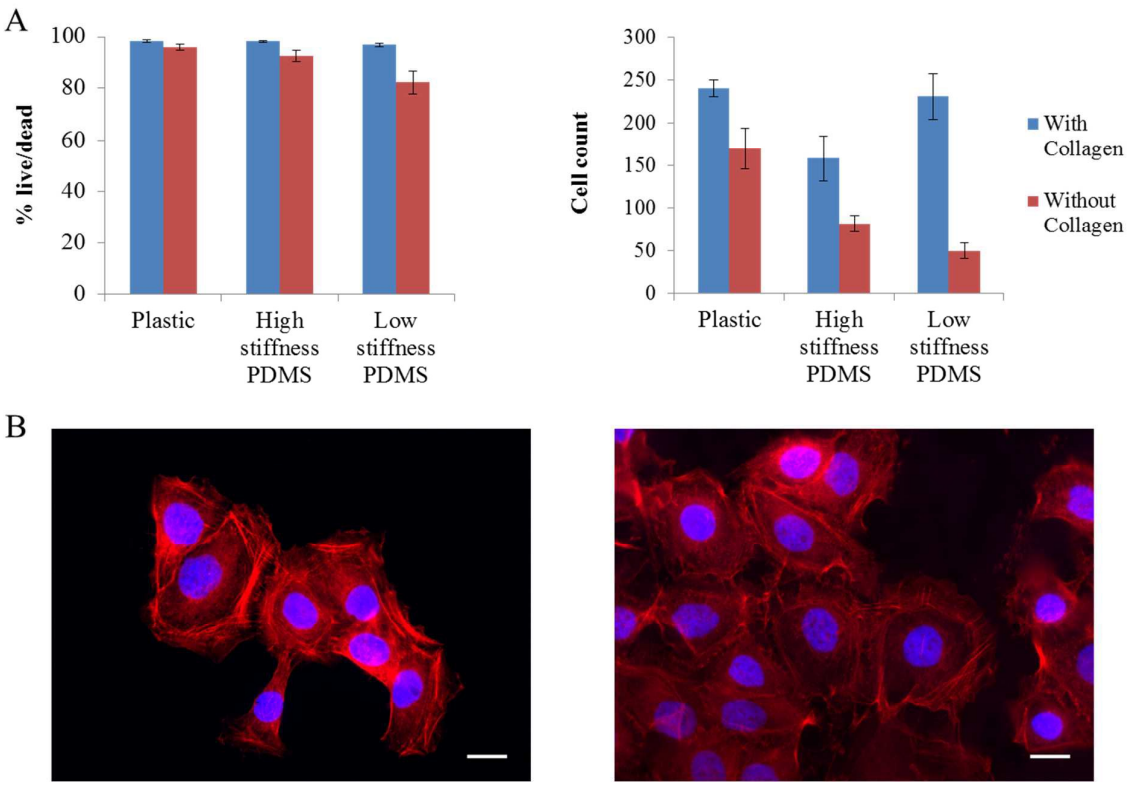

Fig. 7 Cytocompatibility of UV cross-linked PDMS**.** A. HaCaT cell viability (10,500 cell/cm^2) when cultured on the cross-linked PDMS at high (126 kPa) and low (5 kPa) storage moduli conditioned with collagen type I (C) (Blue) and without collagen treatment (Red). B. HaCat cell spreading on PDMS at high (Left) and low (Right) stiffness. Scale bar is 10µm.

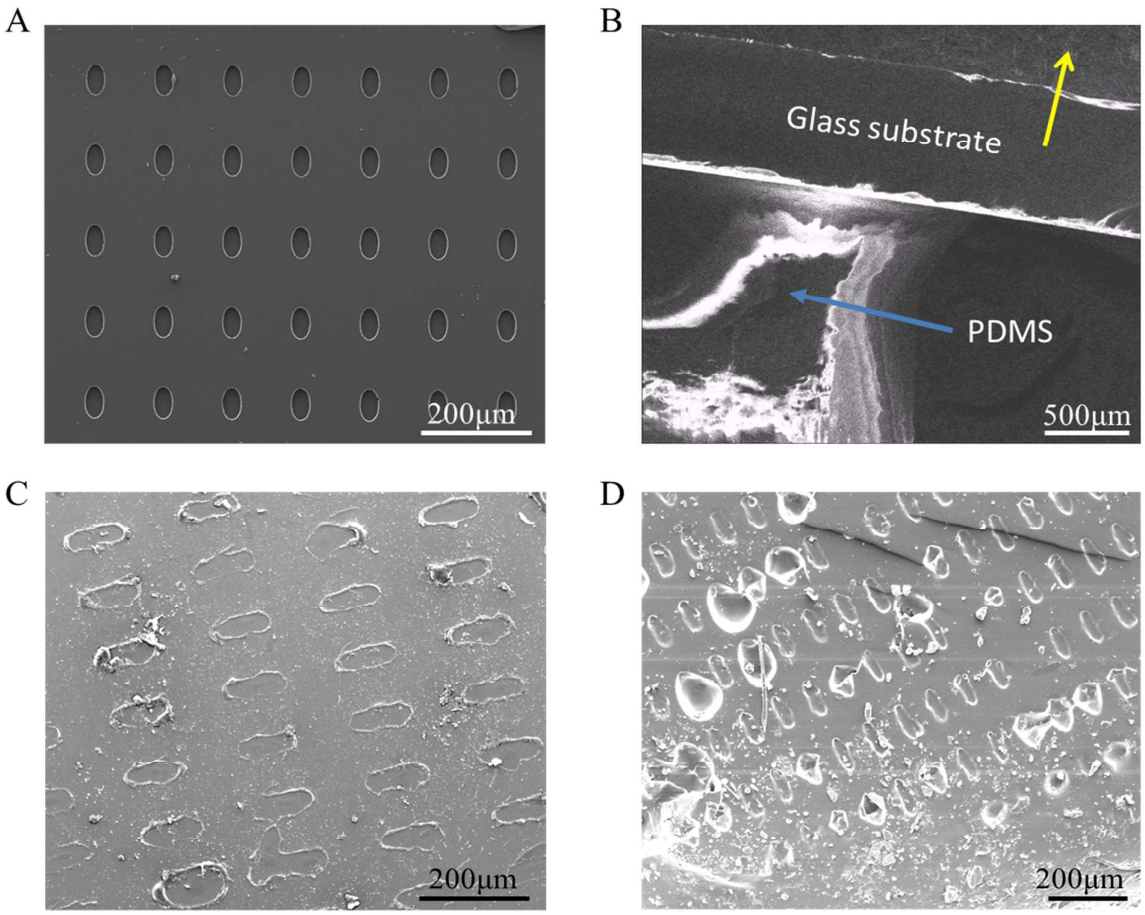

Fig. 8 Ultrafast Diffusion-Controlled Thiol-Ene Based Crosslinking of Silicone Elastomers with Tailored Mechanical Properties for Biomedical Applications A. SEM image of PDMS subtrate after UV curing (94 mW/cm^2) and peeling off from the conventional master revealing a clean and nice pattern (UV curable resin was formulated from alkene:thiol ratio of 1:2 and vinyl-PDMS of 10,000 cSt). B. The deformation of PDMS sample captured *in-situ* (by SEM, top view) during the tensile test (Yellow arrow indicates the pulling direction). The maximum stress at break obtained from this bonding structure was measured as 0.199MPa from stress-strain curves (see Supplementary Fig. S3). The resulting surfaces (glass, C and silicone, D) after fracture clearly show residues associated with cohesive failure.

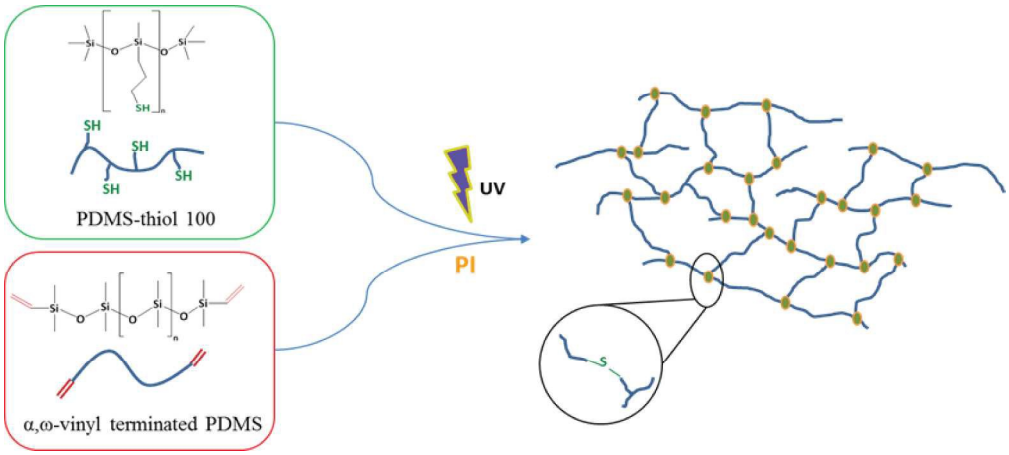

252x112mm (300 x 300 DPI)